# Results from the Fly's Eye Experiment

D.J. Bird,[1,3] S.C. Corbató,[3] H.Y. Dai,[3] B.R. Dawson,[2] J.W. Elbert,[3] T.K. Gaisser,[5] K.D. Green,[3,4] M.A. Huang,[3] D.B. Kieda,[3] S. Ko,[3] C.G. Larsen,[3] E.C. Loh,[3] M. Luo,[3], M.H. Salamon,[3] J.D. Smith,[3] P. Sokolsky,[3] P. Sommers,[3] T. Stanev,[5] J.K.K. Tang,[3] S.B. Thomas,[3] S. Tilav [5,6]

[1]*Department of Physics, University of Illinois at Urbana-Champaign, Urbana, IL 61801 USA*

[2]*Department of Physics and Mathematical Physics, University of Adelaide, Adelaide, South Australia 5005 Australia*

[3]*High Energy Astrophysics Institute, Department of Physics, University of Utah, Salt Lake City UT 84112 USA*

[4]*Present address: Department of Physics, The University of Michigan, Ann Arbor, MI 48109 USA*

[5]*Bartol Research Institute, University of Delaware, Newark DE 19716*

[6]*Present address: Department of Physics, University of Wisconsin, Madison, WI 53706 USA*

## Abstract

We report recently analyzed results on the energy spectrum, and composition of cosmic rays above 0.3 EeV. We observe a break in the spectrum at 3 EeV and a changing composition. The results can be explained by a simple two component model: galactic cosmic rays dominated by heavy primaries and an extragalactic component dominated by light primaries. The observed isotropic arrival direction distribution is consistent with the predictions of this model. A 320 EeV event was also recorded.

## Introduction

The atmosphere acts as an absorber for cosmic rays. For incident energy above about 0.1 PeV, the particle cascades initiated by cosmic rays have enough energy to penetrate the atmosphere and reach the ground with sufficient particles for detection. Because the flux of cosmic rays above 0.1 EeV is about 1 event $km^{-2}hr^{-1}sr^{-1}$ and decreases as the second power of energy, most of the cosmic ray detectors are sparsely spaced ground-based counters covering many square kilometers. By sampling the lateral particle density and measuring the relative arrival time in that sample, the energy and the arrival direction of each cosmic ray can be derived.

It was known in the nineteen fifties that nitrogen molecules fluoresce upon bombardment by charged particles. The fluorescent light is produced mostly in the near UV and

blue region.[1] Oda and others [2] pointed out that a cosmic ray cascade (known as an extensive air shower) in the atmosphere would cause the air to glow along the path of the cascade. A detector made to observe the air glow induced by cosmic ray showers would be able to observe, event by event, the entire longitudinal cascade being developed in the atmosphere, a feat that ground arrays are unable to achieve. This detector would be able to use the atmosphere as a calorimeter, would be sensitive to all cosmic rays regardless of their incident angles and composition, and is suitable for detecting cosmic ray showers from a distance. This technique was developed at Utah [3] and, as a result, the Fly's Eye Detector was built.

## Fly's Eye Detector

The Fly's Eye Detector [4] consists of a pair of detectors separated by 3.4 kilometers: Fly's Eye I and II (FEI and FEII). FEI has 67 1.5 meter diameter front surfaced F/1 mirrors. These mirrors are placed so that they provide complete sky coverage. Placed at the focal plane of each mirror are 14 hexagonal photomultiplier tubes, each of which covers about 5.5°x 5.5°. A gaussian filter (peak transmission of 82% at 356 nm and FWHM= 75nm) is placed in front of each photomultiplier tube. This filter reduced the night sky light by a factor of 10, while reducing the fluorescent signal strength by about 40%. FEII has 36 mirrors and covers $\pi$ steradians in the direction of FEI. Each detector collects data independently of the other. But upon the detection of an event, Fly's Eye I sends a signal to Fly's Eye II electronics, which provides a marker for those events which are simultaneously measured by both detectors.

The determination of the shower plane is a first step toward ascertaining the incident cosmic ray arrival direction. The shower detector plane is the plane determined by the direction cosines of all the photomultiplier tubes in that event. For events observed by both detectors, the arrival direction is given by the intersection of the two shower detector planes. For events observed by one detector alone, the timing of the tubes and the detector plane coordinates determine the arrival direction of the primary cosmic ray. After the track arrival direction and the impact parameter (the perpendicular distance from the track to the detector) are determined, we calculate the longitudinal shower profile. By integrating the shower profile, we obtain the incident cosmic ray energy.

Events observed simultaneously by both FEI and FEII detectors were used to determine the energy resolution of the detectors. Figure 1 shows a histogram of the energy difference divided by the average energy of the two detectors. E1 is the energy from FEI using information entirely from that detector, and similarly E2 is from FEII. Notice that even though the two Eyes have different solid angle coverage which contributes to different track lengths, the systematic energy difference is about 2%. This distribution has a $\sigma$ below 2 EeV of 0.47 and 0.40 above 2 EeV. The energy resolution for events reconstructed using one Eye information only (monocular analysis) is 0.33 below 2 EeV and 0.28 above 2 EeV. A similar method was used to determine the stereo energy resolution. For this estimation, pulse height information from each of the detectors, together with the stereo geometry were used to determine the energy of the event for each detector. The stereo energy resolution was found to be 0.24 above and 0.20 below 2 EeV. Atmospheric attenuation, fluorescent efficiency, calibration uncertainty, effect of random distortions of

**the images, and survey uncertainties contribute to the systematic energy error which is estimated to be about 20-30%.**

## Differential Energy Spectrum and Cut-off

Figure 2a shows the Monte Carlo modelled exposure for Fly's Eye I . Figure 2b shows the exposure for stereo measurement. The difference is attributed to the fact that FEI has twice the solid angle coverage of FEII, only part of the FEI aperture would be detectable from FEII, and was turned on much earlier than FEII. It is interesting to note that both the stereo and monocular exposures increase smoothly as a function of energy and level off above 10 EeV. This shape reflects the way the detector works: the higher the energy the larger the detector collection area becomes. The growth is eventually limited by the exponential attenuation of light in the atmosphere and the shortness of track length for reconstruction.

Figure 3 shows the differential energy spectrum [5] obtained via the stereo detection scheme. A cut in $\frac{\Delta E}{E}$ of 1 has been imposed. First of all, we have multiplied the differential energy spectrum by $E^3$ to flatten it for easy viewing. We observe a change or a break in the slope of the spectrum. Our results show that the slope before 3 EeV is -3.27± 0.2 and after 3 EeV is -2.71 ±0.1.

Figure 4 shows the differential energy spectrum measured by FEI alone. [6] The slope change in the monocular analysis is less pronounced and is shifted to high energy. The difference between the two spectra is due to the difference in the energy resolution of the two methods of observation (The monocular energy resolution is about a factor of 1.5 larger than the stereo resolution). We are able to replicate the monocular spectrum using the stereo spectrum as the input.

In simple words, for a spectrum with a very steep slope, a break in the spectrum is smeared out and pushed to higher energy by a detector with poorer resolution.

We have observed one event above 80 EeV. Using the stereo spectrum from 3 EeV to 50 EeV and assuming that the shape of the spectrum continues above 100 EeV, we predict that we should have seen 6 events above 100 EeV. Instead we have recorded only 1 event. The monocular spectrum shows a lack of events above 100 EeV, a feature which is indicative of a cut-off above 100 EeV. The AGASA array with approximately the same exposure time also detected one event above 100 EeV.[7] Caution must be exercised to combine data from different detectors, especially from two detectors that work on two different techniques. For that and other reasons, we are carrying out a joint calibration program with the AGASA people to understand how a uniform energy scale can be established. The lack of events above 100 EeV is the second new feature of our spectrum result.

To understand the shape of the differential energy spectrum, one must consider the injection spectrum and the effect of transporting cosmic rays through space would have on the spectrum. To illustrate this problem, I pointed to the fact that the 2.7°K microwave photons which have a blackbody distribution will degrade the protonic component of cosmic rays above 50 EeV through photoproduction. Cross sections for single pion and multiple pion production at and beyond threshold have been carefully measured many

years ago. For protons (we will address complex nuclei later) produced beyond 50 EeV, the energy spectrum at detection will depend on the distance travelled. Greisen [8], independently Zatsepin and Kuz'min [9] first mentioned the moderating effect transportation has on the shape of the spectrum. Since then, a number of authors (Hill and Schramm [10] , Yoshida et al. [11], and Elbert and Sommers [12] ) worked out spectrum dependency on energy and distance. Results indicated that by studying the shape of the spectrum with a detector of fine energy resolution, one can study the spatial distribution of the highest energy sources. In virtually all the acceleration models, complex nuclei could also be accelerated to our energy region. In this case, the transportation problem is more complex because complex nuclei are fragmented by the so-called giant dipole resonance process. One not only needs to take interaction between cosmic rays with the 2.7°K radiation into account, but one must also take the radio and infrared photons into account as well. This problem was first worked out by Stecker [13], and lately refined by Elbert and Sommers [12]. Figures 5a,b,c are taken from a paper by Elbert and Sommers. These figures show the integral spectra at detection as a function of the distance the cosmic ray travelled. They used an injection spectrum with index of -2.5 for protons, carbon nuclei, and iron nuclei. I must point out that the distance shown on the graph is not the line of sight distance to the source but the actual distance the cosmic rays travelled. This distance is usually much longer than the line of sight distance, as the extragalactic magnetic field causes all charged particles to take on curved trajectories. Extragalactic magnetic measurements are sparse since they are very difficult to measure. By measuring cosmic rays around 100 EeV, one could use them to probe the magnetic field strength and direction.

## Composition

The Fly's Eye Detector can be used to indirectly measure the cosmic ray composition. For this measurement, we use the so-called shower maximum method. I will give a qualitative description of this method and leave all the quantitative discussions for Tom Gaisser to make, since he, Todor Stanev, and S. Tilav [14] developed a Monte Carlo cascade program with which the chemical composition determination was made. Briefly, for fixed incident energy the larger the total inelastic cross section the higher the cascade will start in the atmosphere and the higher the shower maximum will be in the atmosphere. Heavy primaries tend to fragment. Each fragment possesses lower energy. Thus, for fixed energy, heavy primaries tend to develop early in the atmosphere. Figure 6 shows shower maximum distribution of stereo events as a function of incident cosmic ray energy together with two sets of simulation results. The upper curve is the modelled shower maximum distribution for a pure proton source. The bottom is a modelled curve for pure iron source. Our data indicate that cosmic rays near 0.1 EeV are dominated by heavy primaries. The composition evolves to a lighter composition as a function of energy.

## Extragalactic Cosmic Rays

We propose that cosmic rays are of two components shown below:

$$Iron\ flux:\ log(J(E)(m^2\ s\ sr\ eV)^{-1}) = 33.185 - 3.496 \times log(E) \quad (1)$$

$$Proton\ flux:\ log(J(E)(m^2\ s\ sr\ eV)^{-1}) = 16.782 - 2.610 \times log(E) \quad (2)$$

Using the two components, we are able to simulate results which agree with our stereo data (See Figure 7) as well as with our composition data (see open diamond points in Figure 6).

## The Highest Energy, 320 EeV, Event

A 320 ± 38 (statistical) ± 85 (systematic) EeV event was observed on the 15th of October 1991 at 7:34:16.443 Universal time. [15],[16] Its arrival direction is declination 48.0 ± 6° and right ascension 85.2 ±0.5° (b=9.6, l=163), and landed at the blind spot of Flys Eye II. So it was observed by Fly's Eye I only. The analysis which assumes c, speed of light, as the speed of the shower gave the shower profile shown in Figure 8. To make sure that a 51 joules event was not a micrometeor, Kieda [17] performed an analysis in which the speed of the shower was allowed to vary. He found that the lack of parallax in the track indicated that this track could not have been closer than 500 meters from Fly's Eye I. At that distance, FEII would have seen this event in such a small number of tubes that the event would have failed the trigger requirement. In this case, the low shower speed limit is set at 0.05c. This track could not have been travelling faster than 0.2c. At that speed the track would have been detected by Fly's Eye II. Within this speed range, Kieda [17] found the track has a large zenith angle, and the maximum light is deposited at atmospheric depths of 2000 g cm$^{-2}$. The lack of shower luminosity before this depth and the sudden burst of luminosity are not the normal behavior of dust grains or meteorites which glow as they enter the atmosphere. Furthermore, there is no indication that any part of the object fragmented into slower components, which is not typical of dust particles and meteorites. By these arguments, we believe that the shower was not a dust particle or a meteorite .

Axford [18] postulated that cosmic rays traversing many supernova shocks are capable of reaching this energy. Biermann et al. [19] indicated that AGN's with radio lobes are possible acceleration candidates for this event. A search was performed to locate these sources within a radius of 30 Mpc.

The following sources were identified:

| Sources Galaxy | LoSD | Type of Object | Angle | Acceleration Mechanism |
|---|---|---|---|---|
| M87 | 20 Mpc | AGN with Giant Lobes | 90° | Biermann |
| Cen A | 3-5 Mpc | Galaxy of Large Extent | 135° | Probably Biermann |
| M82 | 3 Mpc | Star Burst Galaxy | 47° | Axford |

LoSD - line of sight distance

Knowing the Galactic field is about 2 microgauss, and that it extends over the thickness of the galactic disk, we calculate that this field will contribute about 8 degrees of bending angle to an iron nucleus, and about 2 degrees to a carbon nucleus. Using the figure from Elbert and Sommers, even from distance of 4 Mpc, heavy nucleus flux such as iron and carbon would be attenuated by a factor of ten in that distance. Figures 5a,b,c would suggest that it is possible for protons to come from either M87 or M82 provided the magnetic field is stronger that 50 nanogauss in the region between M87 and and 150 nanogauss between M82 and the Earth respectively. Schramm et al. [20] indicate that such field values are too large, and the origin of this event remains a puzzle.

*Acknowledgements.* We are indebted to Colonels Frank Cox and James King and the staff of the Dugway Proving Grounds for their continued cooperation and assistance. This work has been supported in part by the National Science Foundation and the U.S. Department of Energy.

## References

[1] P. L. Hartman, Planet. Space Sci. 16, 1315 (1968)

[2] K. Suga, 5th InterAmerican Seminar on Cosmic Rays, La Paz (1962). In which he documented that the idea of using air fluorescence to detect cosmic ray showers was first proposed by M. Oda in 1957.

[3] H. E. Bergeson, G. L. Cassiday, T. W. Chiu, D. A. Cooper, J. W. Elbert, E. C. Loh, D. Steck, W. J. West, J. Linsley, and G. W. Mason, Phys Rev Letters 39, 847 (1997).

[4] R. M. Baltrusaitus et al., NIM A240, 410 (1985).

[5] D. J. Bird et al., Phys. Rev. Lett. 71, 3401 (1993).

[6] D. J. Bird et al., ApJ 424, 491 (1994).

[7] Private communication.

[8] K. Greisen, Phys. Rev. Letters 16, 748 (1966).

[9] G. T. Zatsepin and V. A. Kuz'min, Sov. Phys. JETP Lett. 4, 78 (1966).

[10] C. T. Hill and D. N. Schramm, Phys Rev. D31, 564 (1985).

[11] S. Yoshida and M. Teshima, Prog Theo. Phys 89, 833 (1993).

[12] J. W. Elbert and Paul Sommers to be submitted to ApJ.

[13] F. W. Stecker, Phys. Rev 180, 1264 (1969).

[14] T. K. Gaisser et al., Phys. Rev. D47, 1919 (1993)

[15] D. J. Bird et al., paper submitted to Nature.

[16] D. J. Bird et al., paper submitted to ApJ.

[17] David Kieda, private communication.

[18] W. I. Axford, Astrophysical Aspects of the Most Energetic Cosmic Rays, ed. M. Nagano and F. Takahara (World Scientific, Singapore, 1991) 406.

[19] J. P. Rachen and Peter Biermann,Preprint 510, Januar 1993, Max-Planck-Institut fur Radioastronomie, Bonn, Germany.

[20] G. Sigl, D. N. Schramm, and P. Bhattacharjee, submitted to Astroparticle Physics.

## List of Figures

Figure 1 Histogram of the energy difference divided by the average energy of the two detectors. E1 is the energy from FEI using information entirely from that detector, and similarly E2 is from FEII.

Figure 2a Monte Carlo modelled exposure for Fly's Eye I . Figure 2b Monte Carlo Modelled exposure for stereo measurement.

Figure 3 Differential energy spectrum obtained via the stereo detection scheme. Using the dotted line, obtained by fitting data up to log(E) of 18.5, we predict 230 events above log(E) 18.5. The observed number is 281, a 3.4 $\sigma$ excess.

Figure 4 Differential energy spectrum measured by FEI alone. The slope change in the monocular analysis is less pronounced and is shifted to high energy.

Figures 5a,b,c Integral flux reduction factors shown as a function of energy after a spectrum with differential spectral index of 2.5 has been propagated the indicated distance. Figures 5a, 5b, and 5c are for protons, carbon, and iron respectively.

Figure 6 Average shower maximum distribution as a function of the log of energy in EeV. The upper curve, open squares, is a simulated proton shower maximum distribution based on QCD Pomeron model. The bottom curve is a simulated iron curve based on QCD Pomeron model. Filled circles are data. Open diamonds are determined from the two-component assumption of cosmic rays.

Figure 7 Two component fit to the stereo data. Black circles are data, open diamonds are the superposition of the two components.

Figure 8 Shower profile of 320 EeV event, i.e. the number of particles in the shower as a function of the atmosphere thickness (in g $cm^{-2}$) the shower traversed.

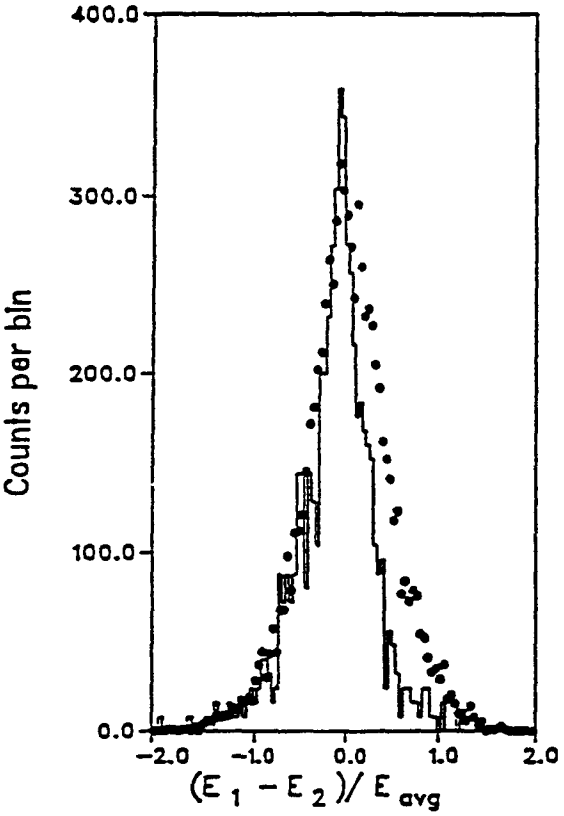


Figure 1.

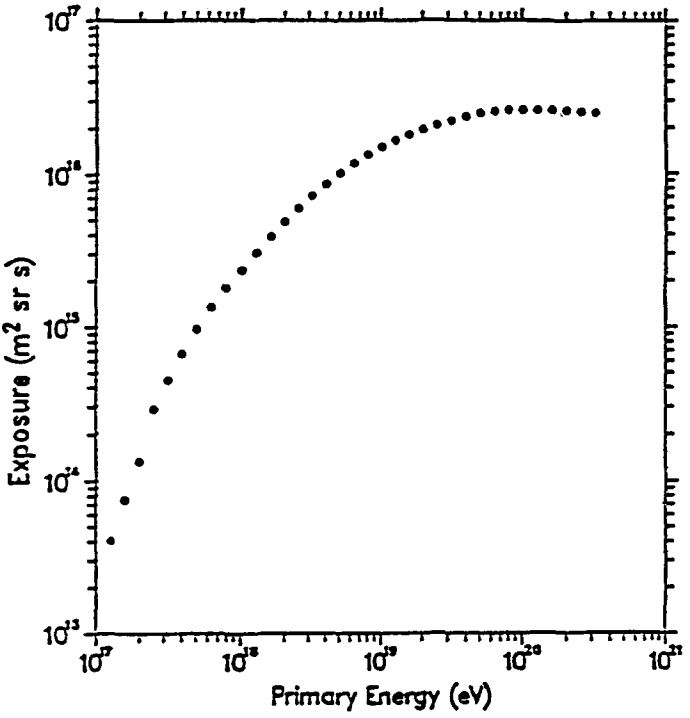


Figure 2a.

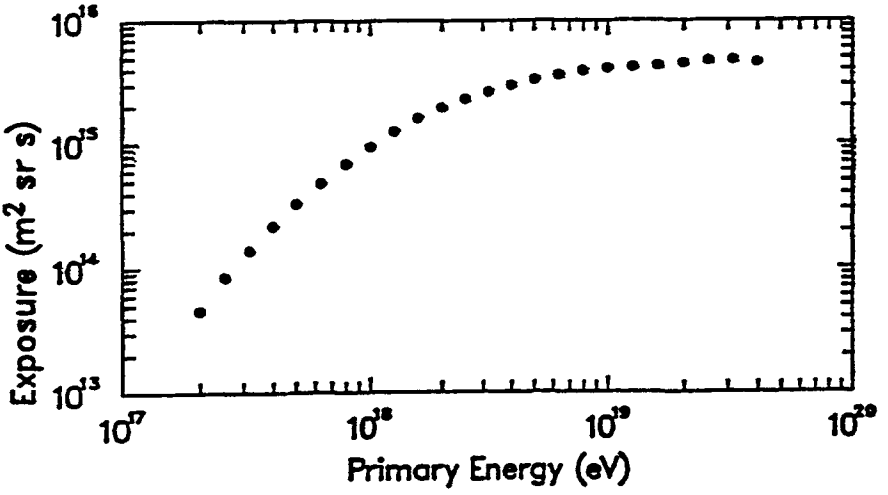


Figure 2b.

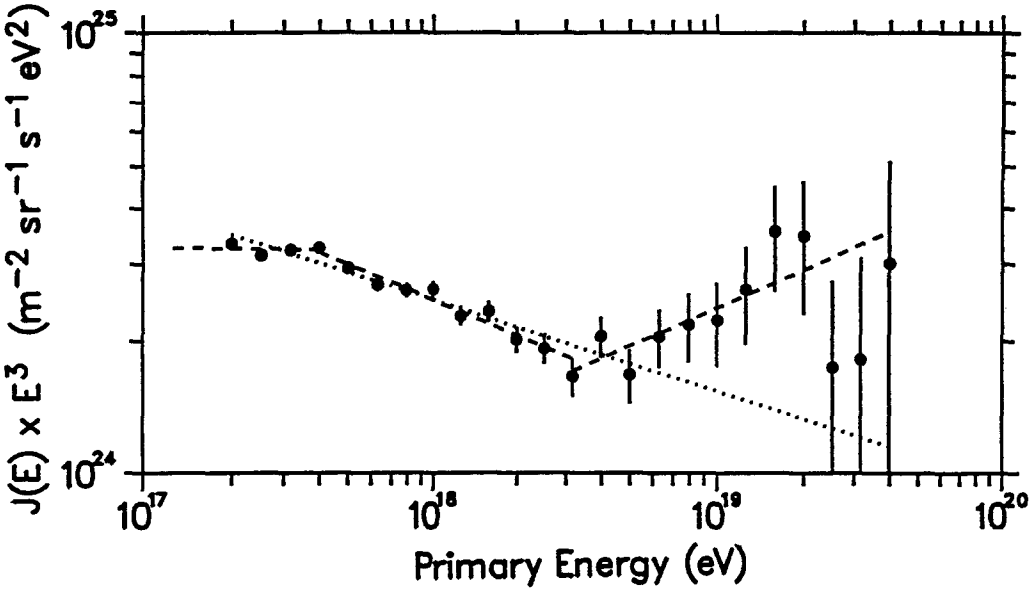
J(E) x E3 (m-2 sr-1 s-1 eV2)
10^25
10^24
10^17
10^18
10^19
10^20
Primary Energy (eV)

Figure 3.

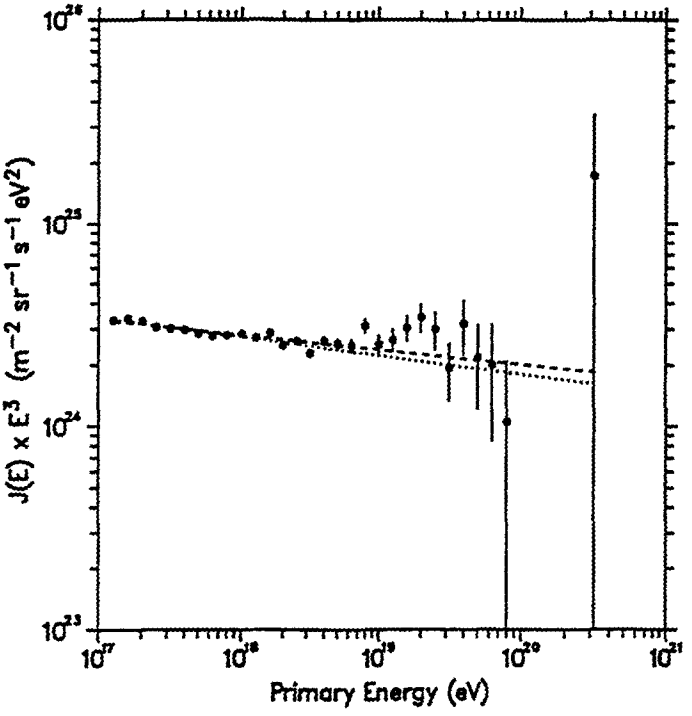
$10^{26}$
$10^{25}$
$10^{24}$
$10^{23}$
$J(E) \times E^3$ $(m^{-2}\ sr^{-1}\ s^{-1}\ eV^2)$
$10^{17}$
$10^{18}$
$10^{19}$
$10^{20}$
$10^{21}$
Primary Energy (eV)

Figure 4.

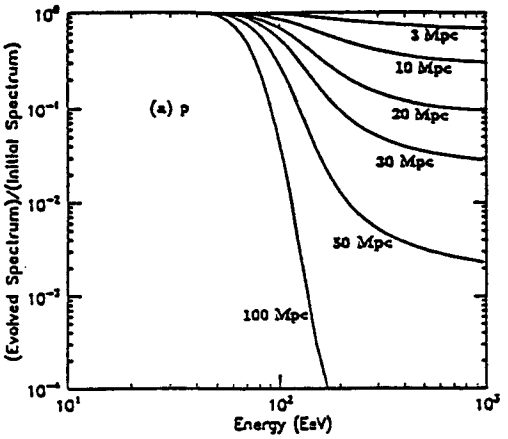


Figure 5a.

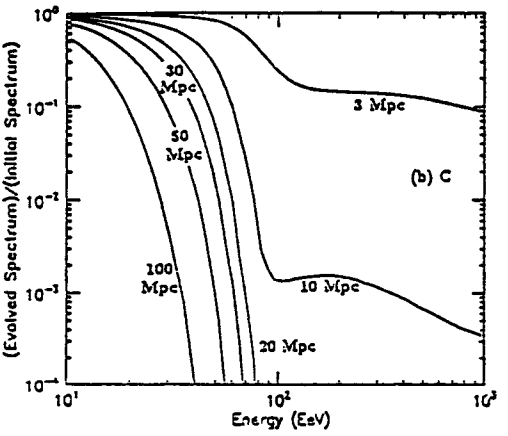


Figure 5b.

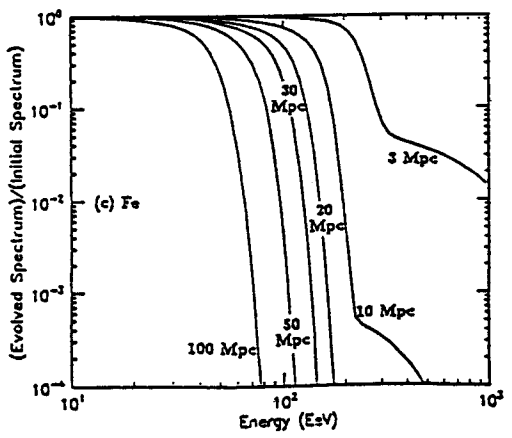


Figure 5c.

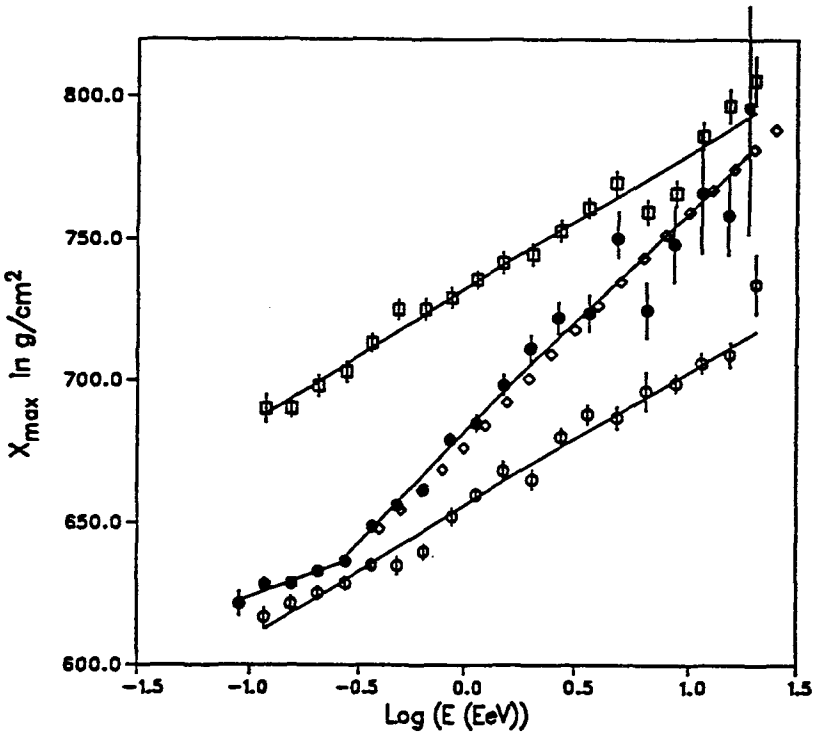
800.0
750.0
700.0
650.0
600.0
$X_{max}$ ln g/cm$^2$
−1.5
−1.0
−0.5
0.0
0.5
1.0
1.5
Log (E (EeV))

Figure 6.

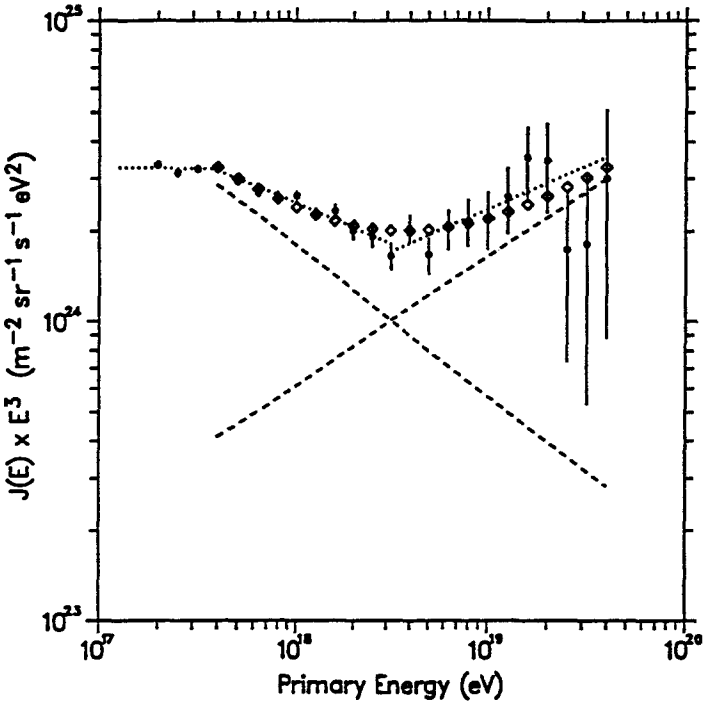
$10^{25}$
$10^{24}$
$10^{23}$
$J(E) \times E^3$ $(m^{-2}\,sr^{-1}\,s^{-1}\,eV^2)$
$10^{17}$
$10^{18}$
$10^{19}$
$10^{20}$
Primary Energy (eV)

Figure 7.

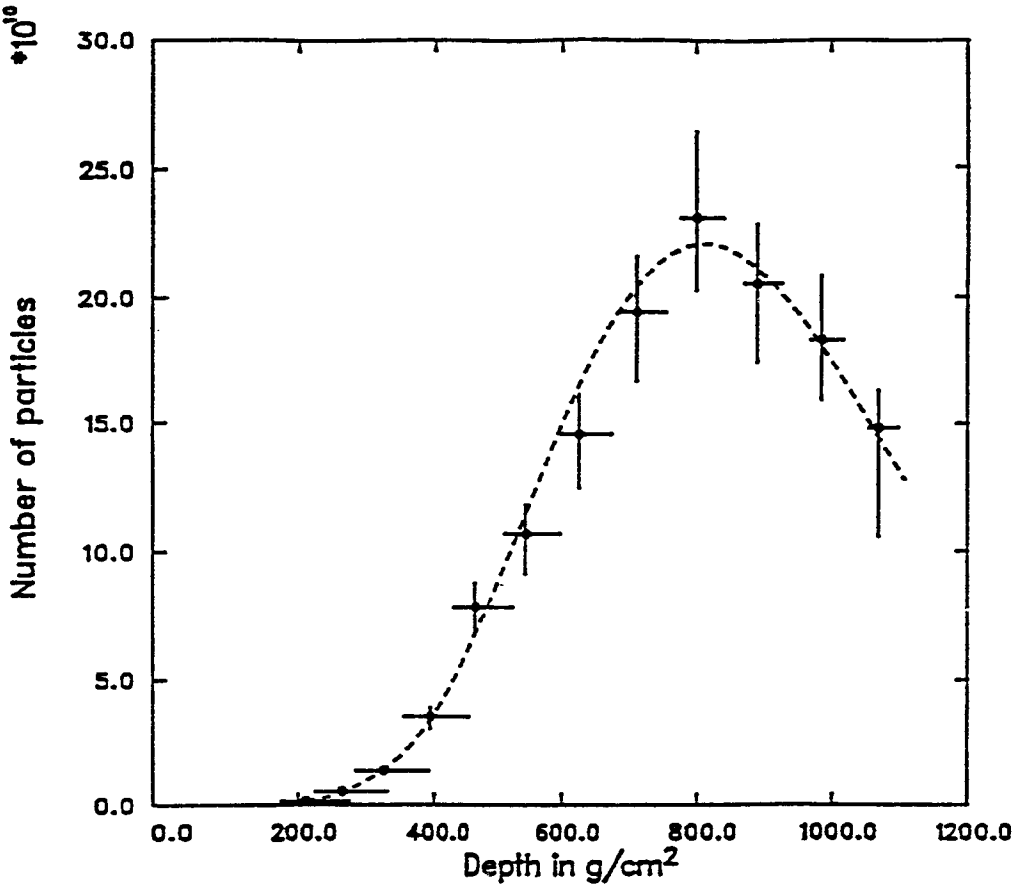
*10^10
30.0
25.0
20.0
15.0
10.0
5.0
0.0
Number of particles
0.0
200.0
400.0
600.0
800.0
1000.0
1200.0
Depth in g/cm^2

Figure 8.